FAILURE ANALYSIS OF ADHESIVELY BONDED JOINTS CONSISTING OF BI-LAYER COMPOSITES

M. S. Kim[1*], C. Y. Park[1] and S. M. Jun[1]
[1] Agency for Defense Development, Daejeon, Korea
*castle@add.re.kr

Keywords: *Double Cantilever Beam, Conformal Load-bearing Antenna Structure, Bonded Joints, Adherend, Cohesive Zone*

1. Introduction

The 5th generation fighter aircraft has been known as its invincible super-cruise, invisible external shape, and low observable radar cross section area. Lots of technologies for undetectable functions were gathered to make outstanding stealth functions. One of those technologies for stealth aircraft is embedded antenna structure technology. Broadband or multiband antenna is embedded in the skin of an aircraft structure that carries aerodynamic load. The embedded antenna structure has advantages of lower weight, reduced drag, efficient aircraft maneuver, greater flexibility in locating antennas, cost saving, and reduced number of antennas, etc, in addition to the stealth function. The antenna also deforms together with the skin deformations maintaining antenna performance. This multi-functional embedded antenna structure is called Conformal Load-bearing Antenna Structure (CLAS).

CLAS is made of multi-layered composites; each layer has different material properties. The interfaces of these layers are connected using adhesively bonded joints. The failure strength of the interfaces is the main issue of design when the CLAS system is subjected to aerodynamic loads. Invisible small cracks, delaminations, and interface debonding of CLAS should be carefully analyzed and predicted. To find out the failure mechanism of multi layered structure(CLAS), this study deals on the bonding strength of bi-layer specimen. With an application of bi-layer specimen we perform the DCB test and numerical calculation to verify the delamination, crack propagation, and failure. The progressive failure analysis using cohesive zone modeling technique was applied for the simulation.

From reviewing the previous researches, several analytical and computational approaches for double cantilever beams(DCB) and adhesive layers or adhesive-adherend interfaced layers can be found. Sridharan and Li studied two distinct cohesive layer models of delamination growth in the DCB. Makhecha *et al.* analyzed a double cantilever beam under dynamic loading using cohesive zone model. Colavito and Madenci distinguished differences of failure strength from two kinds of initial cracks using digital image correlation. Needleman studied progressive failure and crack growth using cohesive elements. Other adhesive joint researches were carried out recently.

Among the mechanical phenomena of adhesively bonded joints, this study focuses on a progressively failure and crack propagation analyzed by cohesive zone modeling, i.e. cohesive elements. Especially, this study consider adhesively bonded joints when the adherends are made of different materials. To obtain a more fundamental view of fracture in damaged structures, it is necessary to introduce a new concept for a fracture process zone, so called cohesive zone, found in the very weakening bonded joints. In particular, the focus of this paper is the fracture propagation behavior of brittle typed composites that can be characterized taking into account the finite element commercial software; ABAQUS.

To verify the present model of adhesively bonded joints, this study conducts several testing on Glass Fiber Reinforced Polymer(GFRP) and uni-directional Carbon Fiber Reinforced Polymer (CFRP) specimens. The strain and the crack growth shape under quasi-static loading are monitored during the Mode I DCB tests. After obtaining the experimental data and numerical solutions, these results are compared together and then provide a detailed explanation of mechanical behavior of composite specimens.

2. Cohesive Damage Model

The plastic zone around crack tip region has been analyzed using extended finite element method (XFEM), crack tip elements and stress intensity factors, etc. This study introduces cohesive zone model to analyze crack propagation, delamination, and failure of adhesively bonded structure. Needleman suggested a material separation law based on the components of tractions and separations in the cohesive zone and introduced the concept of cohesive surfaces as shown in Fig. 1. The symbol a is initial crack, d is displacement, green zone is cohesive zone that traction forces which is function of infinitesimal displacement Δ move toward normal and tangential directions of x-axis in Fig.1

In this work, the traction separation law of Ref. [3] is applied to analyze the interface behavior. The constitutive behavior of crack tip is represented by defining potential function, $\phi(\Delta_n, \Delta_t)$ of the type where Δ_n and Δ_t are normal and tangential jump. The interface tractions ($\mathbf{T}$) across the cohesive zone surface are given by the surface energy density function per unit un-deformed area.

$$\phi = e\sigma_{\max}\delta_n - e\sigma_{\max}\delta_n e^{(-\Delta_n/\delta_n)}\left[1+\frac{\Delta_n}{\delta_n}\right]e^{(-\Delta_t^2/\delta_t^2)}$$

$$\mathbf{T} = -\frac{\partial\phi}{\partial\mathbf{\Delta}} \qquad (1)$$

In Eq.(1), the variable $\sigma_{\max}$ is used to scale the normal and the shear cohesive stresses, and the characteristic distance of the normal and the shear stresses are assumed to be $\delta_0 = \delta_n = \delta_t$, respectively.

A cohesive damage model is used to simulate crack propagation. The damage model considers a quadratic stress criterion to deal with damage initiation assuming that normal compressive stresses do not induce damage.

$$\left(\frac{\varepsilon_I}{\varepsilon_{u,I}}\right)^2 + \left(\frac{\varepsilon_{II}}{\varepsilon_{u,II}}\right)^2 + \left(\frac{\varepsilon_{III}}{\varepsilon_{u,III}}\right)^2 = 1, \text{ if } \varepsilon_I \geq 0$$

$$\text{And } \left(\frac{\varepsilon_{II}}{\varepsilon_{u,II}}\right)^2 + \left(\frac{\varepsilon_{III}}{\varepsilon_{u,III}}\right)^2 = 1, \text{ if } \varepsilon_I \leq 0 \qquad (2)$$

Crack propagation is defined based on the energy called the fracture energy that is dissipated as a result of the damage process. Damage propagation is simulated using the linear fracture energy based on the quadratic criterion :

$$\left(\frac{G_I}{G_{Ic}}\right) + \left(\frac{G_{II}}{G_{IIc}}\right) + \left(\frac{G_{III}}{G_{IIIc}}\right) = 1 \qquad (3)$$

These two criteria are expressed in terms of relative displacements between homogeneous points of the interface finite element. The fracture energy is specified as a material property shown in Eq. (3). The dependence of fracture energy on the mode can be specified by analytical forms in terms of energies. The critical strain energy release rates for each pure mode loading can be written as

$$G_{ic} = \frac{1}{2}\sigma_{u,i}\delta_{u,i}, \; i = I, II, III \qquad (4)$$

In Eq.(4), the variable $\delta_{u,i}$ means the corresponding relative displacements at the failure under each pure and mixed mode loading. The critical strain energy release rates, $G_{ic}, i = I, II, III$, are obtained from experiments on the mechanical property test. After finding the respective fracture energy of mode I/II/III, the cohesive modeling is applied into the commercial finite element package, ABAQUS to depict the initiation and growth of delamination.

3. Finite Element Implementation

To analyze Mode I fracture strength, a cohesive zone modeling is applied. Cohesive elements of ABAQUS S/W is implemented to depict the cohesive zone area. COH3D8 element with 8 nodes and 4 integration points is appropriate for modeling the bonding adhesive. The thickness of cohesive element can be a finite value or zero. The degree of freedom of nodes is normal translation and two shear movement. The crack growth of the adhesive can be simulated using failure loading of the cohesive element. Bottom and top surfaces are defined using the 8 nodes, and these surfaces open when they reach failure load : two surfaces of cohesive elements separate with each other.

To apply the cohesive model of mode I fracture analysis, we consider a two-layered composite specimen with the initial crack tips to the free end of the specimen. The dimensions of DCB numerical model are width B =18mm, free-length L =120mm and initial crack length a =30mm. The thickness of two layers are h_1=2mm and h_2 =1mm, respectively.

The finite element of DCB specimen has 5,355 brick elements and 7,200 nodes and the adhesive layer has approximately 1,071 eight-node cohesive elements(COH3D8) shown in Fig. 2.

To solve the adhesively bonded bi-layer composites, material properties fitted for structural shape are needed. GFRP/CFRP lamina properties and adhesive properties are shown in Table1 and Table 2, respectively. The stacking sequences of each adherend are the same as [(45/0/-45/90)2]. The structural analysis of damaged composites under ultimate load can verify discontinuous cracks. The load mechanism near the micro crack tip region can also be depicted using cohesive elements. Traction forces and micro displacements in the cohesive elements are used to solve the crack propagation. A number of load steps are diversified to simulate the applied load infinitesimally. Each load step is converged within the maximum iteration number of load steps. So, each load step can be inspected and the detail damage distribution and crack propagation can be checked.

4. Bi-Layer Double Cantilever Beam (DCB) Test

The DCB Test specimen is widely used to verify the characteristics of Mode I fracture toughness. The initial crack is generated to open the pure mode I crack easily and provides larger fracture toughness than the test specimen with a pre-crack

4.1 Bi-Layer Test Specimen of Double Cantilever Beam (DCB) Test

Two specimens made of Glass/Carbon Fiber Reinforced Polymer(GFRP/CFRP) are used to predict the delamination strength of DCB tests. The DCB test specimens are manufactured by adhesive bonding and cured laminates of GFRP/CFRP. The composites are prepared from unidirectional tape and fabric prepreg consisting of intermediate modulus GFRP/CFRP fibers. The composite test specimen has also the same geometry as shown in Fig. 4. The unidirectional tape/woven fabric stacking sequence is a [(45/0/-45/90)2] prepared by 8-plies, and each ply is composed of carbon fiber yarns(T700GC-12K-31E) and glass fiber yarns(STYLE7781). The relevant mechanical properties of the lamina are listed in Table 1. The matrix is TORAY #2510 epoxy resin from TORAY company. After curing the prepreg in the autoclave, the laminate is cut out for a specified specimen size. The ENF specimen is manufactured by attaching the adhesive named HYSOL EA9696. The properties of the adhesive are given in Table. 2.

4.2 Procedures of Bi-Layer Double Cantilever Beam (DCB) Test

A universal testing machine, Material Testing System(MTS)-809, is used to implement the loading of pure mode I direction. The tests are conducted by appropriate apparatuses and prepared according to the procedures and requirements of ASTM D5528-01. The test apparatus for loading the specimen and constituting the boundary conditions are shown in Fig. 4. The load is fulfilled by a displacement control mode at 1 mm/minute. To capture the dynamic image of the crack propagation, a high speed camera is used. The captured image is used to correlate with the load displacement traces to establish crack lengths corresponding with the crack propagation scene. The dynamic scene of crack propagating interlaminar direction is shown in Fig. 5.

The displacement load is applied until the interface of specimen reaches final debonds or delamination of adherends occurs with monitoring the crack growth. When a sudden movement or sound is detected, the test is paused for inspection of the test setup and the specimen during the monitoring. After confirming the normal state of the test setup, the loading was continued until the complete fracture of the bonding line occurs.

4.3 Results of Bi-Layer Double Cantilever Beam (DCB) Test

Two specimens of bi-layer composites are used to conduct the DCB test. Load displacement curves are monitored and recorded during the test while monitoring the test setup. Both of tests are continued until initial crack reaches the opposite side ; the initial crack propagates to the specimen length as shown in Fig. 6(d). Figure 6 shows the dynamic image of final fracture using high speed camera with

1,000 pictures per second. The crack propagates after peak load with load level of 10 Newton as shown in Fig. 6(a)~(c) just before the failure. The displacement in the opening direction is 78 mm which is 65% of the full length at the failure point.

Figure 7 shows load displacement traces of two DCB tests. Test 1 and Test 2 have difference of peak load value as 10 N and the slopes from zero load to the peak load value make some difference. Both curves have typical DCB characteristics of showing minus decrease slope after the steep linear increase to the peak load.

The finite element simulation using cohesive elements show similar trace with the test result. Figure 9 shows simulation of load-displacement curve indicating linear increase A, peak load value B, rapid decrease C, and slanted decrease D. Stress contour plots are also simulated according to the load-displacement curves. Figure 10 shows four stress contour plots that match points A, B, C, and D of Fig. 9, respectively. We can find out that the applied load level is the maximum value when the crack length arrives at the beginning stage. But the peak load shows some discrepancy between the two peak values as shown in Fig. 11. About 33% of the difference of the peak load value originates from inappropriate material properties of GFRP.

8. Conclusion

To characterize the failure of the bonding structure of CLAS system, DCB tests are conducted for mode I failure strength validation. Two kinds of Adherends are used to predict the delamination characteristics of specimens. The first one is made of CFRP and the second one is made of GFRP composites. The initial crack occurs in the specimen as shown in Fig. 2. The bi-layer DCB specimen shows large deflections before final fracture of the bonding line. The crack propagated until the two adherend separate into two parts completely along the bonding line. The crack length displacement curve traces a typical DCB shape. Stress contour plots are well simulated to calculate the crack growth, delamination and failure.

After simulating the crack growth-displacement curves, the curve shape is suitably predict the test result and the value of peak load prediction has some discrepancy between test results.

Mode I test and simulation will be handled with more specimens and reliable material properties, and Mode II, III failure mechanism will be dealt on in the next study.

References

[1] S. Sridharan and Y. Li "*Two Distinct Cohesive Layer Models in Composite Delamination Investigation*". The 48th AIAA/ASME/ASCE/AHS/ASC Structures, Structural Dynamics and Materials Conference, April 23-26 2007, Honolulu, Hawaii, AIAA-2007-1994,

[2] D.P. Makhecha, R.K. Kapania, E.R. Johnson, and D.A. Dillard, "*Dynamic Fracture Analysis of Adhesively Bonded Joints Using Explicit Methods*", The 47th AIAA/ASME/ASCE/AHS/ASC Structures, Structural Dynamics and Materials Conference, May 1-4 2006, Newport, Rhode Island, AIAA-2006-1961

[3] A. Needleman " Micromechanical modeling of interfacial decohesion", *Ultra-microscopy,* Vol.40, No. 3, pp.203-214, 1992

[4] K.W. Colavito and E. Madenci "*Adhesive Failure in Hybrid Double Cantilever Beams by Digital Image Correlation*", The 51st AIAA/ASME/ASCE/AHS/ ASC Structures, Structural Dynamics and Materials Conference, April 12-15, 2010 Orlando, Florida, AIAA-2010-2603

[5] Paul J. Callus " *Conformal Load-bearing Antenna Structure for Austrialian Defense Force Aircraft*" DSTO-TR-1963, Commonwealth of Australia, 2007

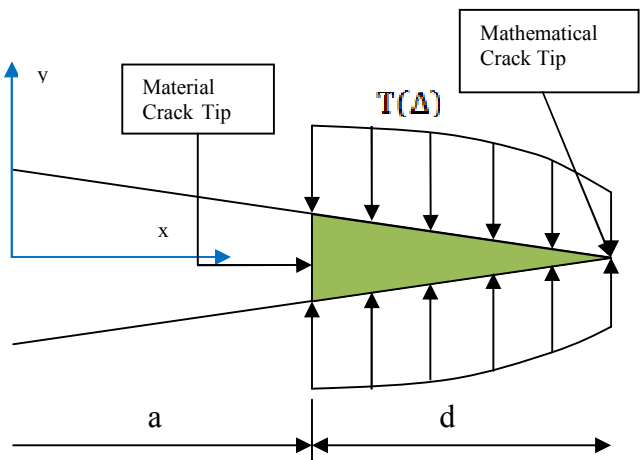

Fig. 1 : Cohesive Zone at the Crack Tip

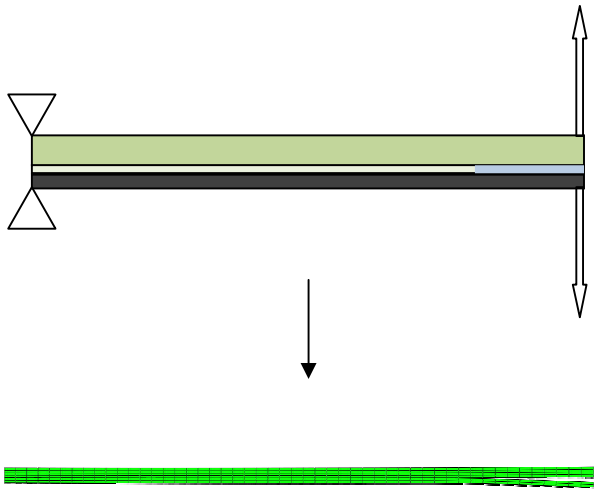

Figure 2 : Double Cantilever Beam

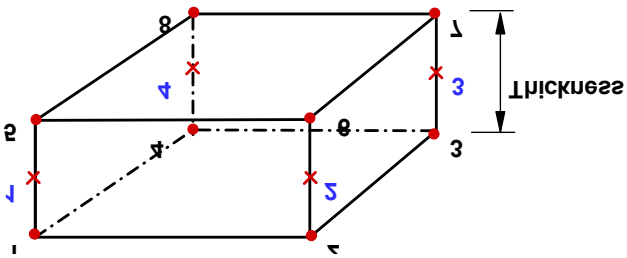

Figure 3: Cohesive Element of COH3D8

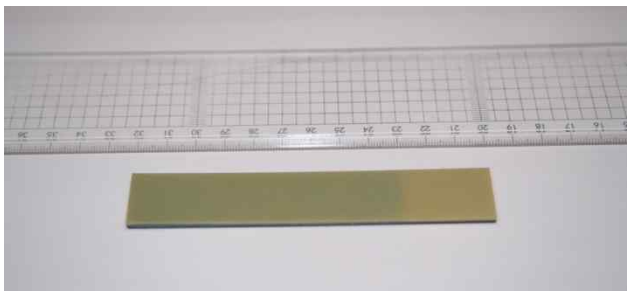

Figure 4 Test Specimen for the DCB Test

Table 1. Material Properties of CFRP/GFRP Lamina

Property	E_{11} (GPa)	F_{tu} (MPa)	ν_{12}	ν_{13}	G_{12} (GPa)	G_{13} (GPa)
P707AG	125	2172	0.3	0.3	4.226	4.226
FGF7781	23.6	442	0.13	0.13	4.37	4.37

Table 2: Adhesive Properties

Property	Test Temperature	Curing Period	Tensile Lap Shear Strength(G_{12})
Hysol EA9696	77°F	60-90 minutes (225°F-265°F)	43.4 MPa

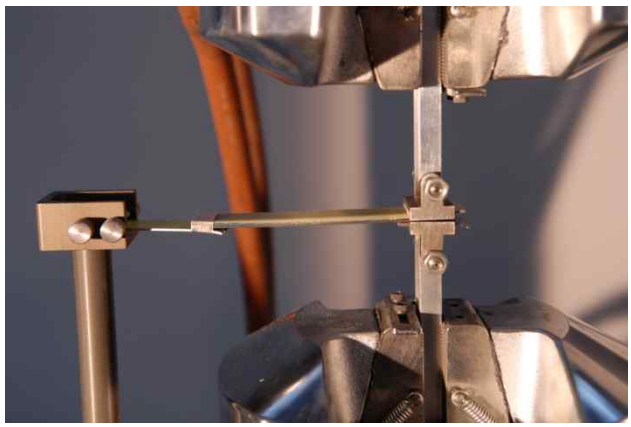

Figure 5 : Testing Apparatus of DCB Tests

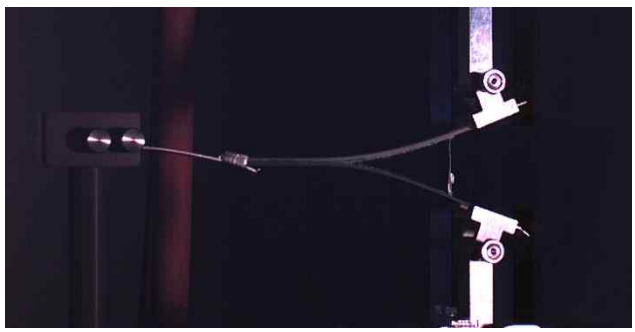

(a)

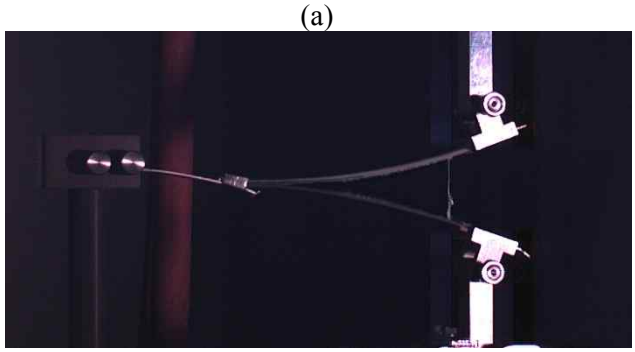

(b)

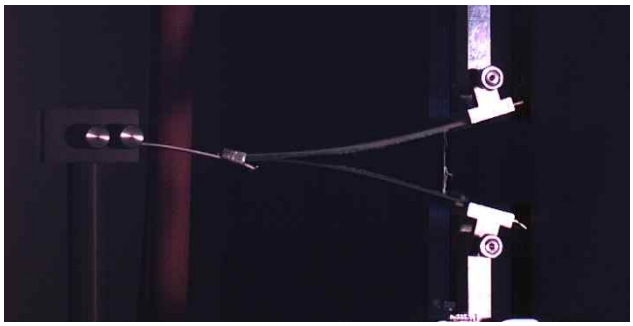

(c)

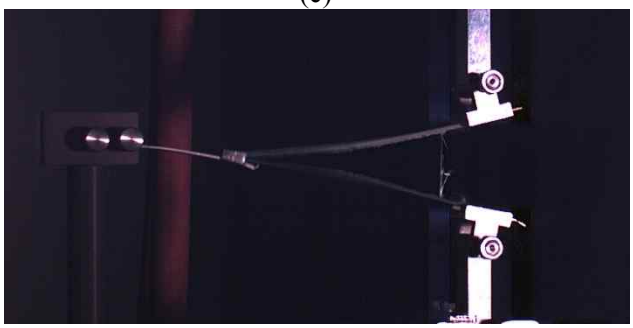

(d)

Figure 6: Video Images of 8-Ply DCB Specimen

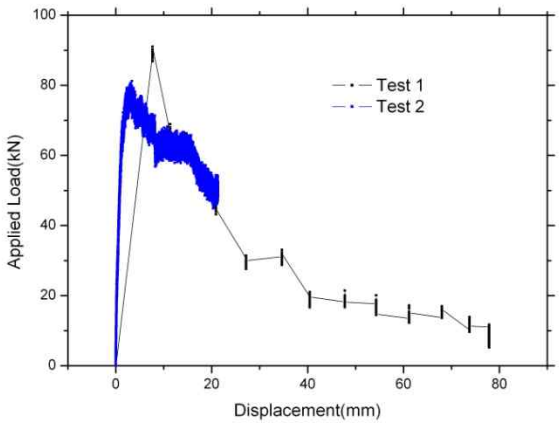

Figure 7: Load Displacement Traces of DCB Tests

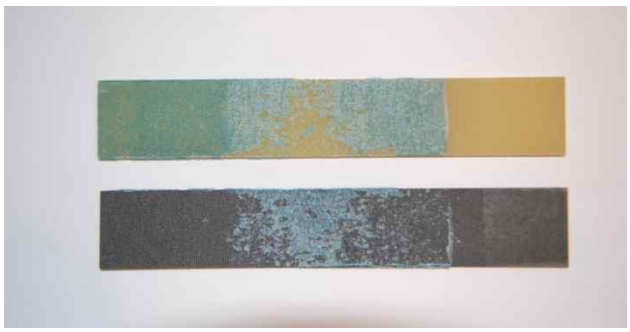

Figure 8: Fractured DCB Specimen

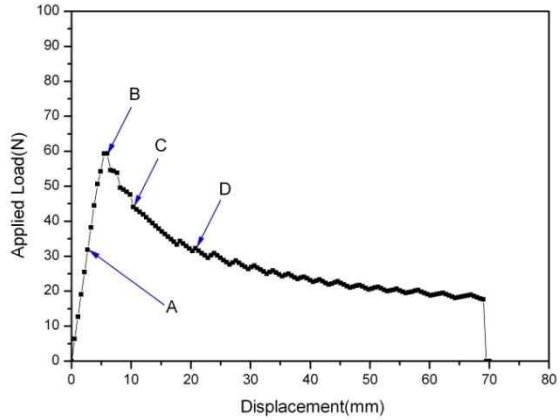

Figure 9: Load Displacement Curves of Analyses

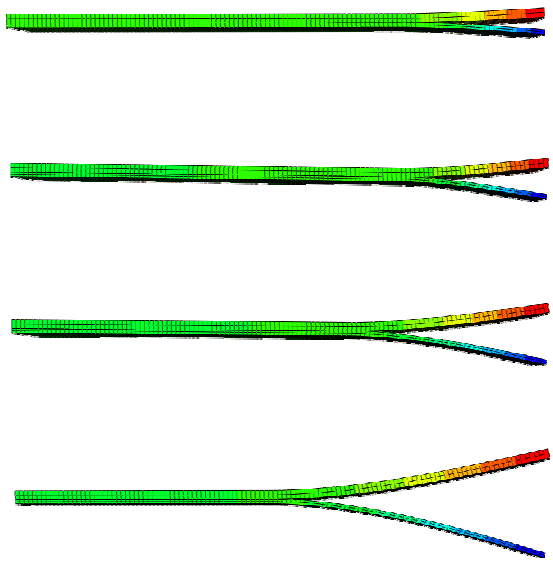

Figure 10: Stress Plots at the Points of A, B, C, and D

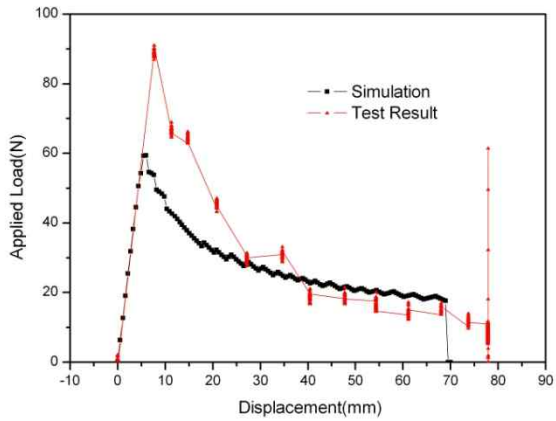

Fig. 11: Comparison Between Tests and Analyses